PHILOSOPHICAL TRANSACTIONS OF THE ROYAL SOCIETY B BIOLOGICAL SCIENCES

Analysis of DNA damage and repair accompanying differentiation in the intestinal crypt

Douglas J. Winton and Roger A. Brooks

Phil. Trans. R. Soc. Lond. B 1998 **353**, 895-902
doi: 10.1098/rstb.1998.0253

The Royal Society

Analysis of DNA damage and repair accompanying differentiation in the intestinal crypt

Douglas J. Winton and Roger A. Brooks

CRC Human Cancer Genetics Research Group, Addenbrooke's Hospital, Box 238, Level 3 Lab Block, Hills Road, Cambridge CB2 2QQ, UK

The ability to process damaged DNA may vary between cells depending on their differentiated status. However, there is little *in vivo* data available and it is not intuitively obvious how the activity of specific repair pathways may vary between different subpopulations (e.g. stem cells and proliferative, committed and differentiated cells) of a particular tissue. To obtain such information for the intestinal epithelium, we have developed an assay that detects differences in the way different regions of the crypt (stem, proliferative and maturation zones) respond to DNA damage. The assay is a variant of the 'comet' assay, which detects DNA strand breaks by measuring the proportion of DNA migrating from individual cells, or in this case intact isolated crypts, in an electrophoretic field. The method is quantitative, with the amount of migrating DNA being proportional to the number of strand breaks. Isolated crypts are repair competent and spatial differences are apparent with some agents. The assay has the potential to characterize the repair properties of cells at different stages of differentiation within the crypt, determine the characteristics that might predispose them to damage and may help in understanding the route of stem cell mutation.

Keywords: intestine; crypt; DNA repair; mutation; differentiation; comet assay

1. INTRODUCTION

It is unclear why cancers affecting some tissues are more common than others. This is best illustrated in experimental animals where carcinogen treatment or a specific genetic deficiency can result in a tissue-specific pattern of tumour formation (Ito *et al.* 1991; Harvey *et al.* 1993, 1995; Hu *et al.* 1994; Jacks *et al.* 1994; Purdie *et al.* 1994).

The aetiology of cancer is multifactorial and some factors may favour tissue-specific carcinogenesis in an identifiable or calculable way by increasing the frequency of somatic mutations. Examples of these would include routes of absorption/excretion; pathways of metabolism or direct exposure to environmental (or experimental) genotoxins; or the number of steps associated with neoplastic transformation. However, additional factors are associated with complex tissue responsiveness after injury, which makes any rationalization of outcome in terms of cancer development difficult. Examples of these include the presence and relative activities of individual DNA repair pathways, induction of apoptoses and cell cycle checkpoints. The balance between these processes provides the major determinant of the frequency of induced mutations after genotoxic injury.

For cellular mutations to have a role in the subsequent development of neoplastic disease they need to occur in long-lived proliferative or stem cells. In most renewing tissues, stem cells are spatially separated from their differentiated descendants (Potten *et al.* 1979). Therefore the spatial pattern of occurrence of cellular events relevant to mutation is important. It is partly for this reason that the intestinal epithelium provides an ideal model for the study of tissue responses after genotoxic injury. In intestinal epithelium the differentiated and functional cell compartments are present as a simple columnar epithelium on intestinal villi; they are physically separated from the stem cells, which are situated towards the bottom part of intestinal crypts.

2. IMPORTANCE OF DNA REPAIR

In mouse intestinal epithelium, somatic mutation assays based on endogenous marker loci, such as *Dlb-1* or *G6PD*, or transgenic shuttle vectors can be used to estimate mutational load. Using these assays, many direct-acting genotoxins and carcinogens requiring metabolic activation have been demonstrated to be potent intestinal mutagens. The importance of DNA repair activities in determining intestinal mutational load after exposure to genotoxins has been demonstrated using the *Dlb-1* assay. For example, irradiation of mice at high and low dose rates (1.8 and 0.1 Gy min^{-1}) both induce *Dlb-1* mutant clones in a dose-dependent manner (Winton *et al.* 1989). However, at the lower rate of delivery there is a dose sparing effect such that fewer mutants are induced for each gray of dose (7.7 versus 4 mutant clones per 10^5 crypts per gray for high and low dose rate, respectively) (figure 1). Comparable evidence for dose sparing with decreased dose rates come from *in vivo* survival (clonogenicity) assays in which ablation of most stem cells by large total doses of irradiation is followed by the formation of microcolonies from regenerating surviving cells (Fu *et al.* 1975; Huczkowski & Trott 1984).

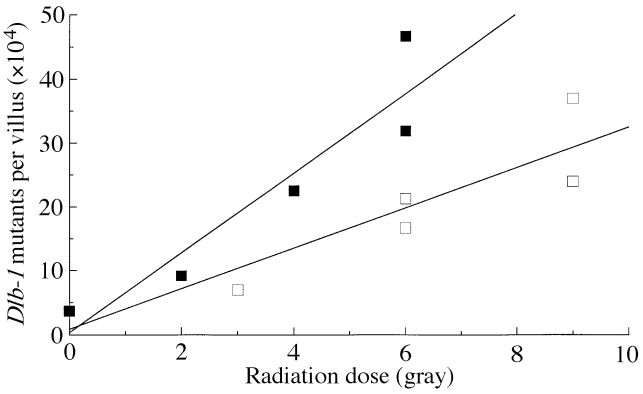

Figure 1. Dose sparing effects in the induction of *Dlb-1* mutants by gamma irradiation at high (1.8 Gy min^{-1}) or low (0.01 Gy min^{-1}) dose rates. Each data point is the mean of six mice analysed for *Dlb-1* mutants as described previously (Winton *et al.* 1989). Lines were fitted by least squares regression (correlation coefficient, 0.92 for both plots). The slopes describe an induction rate at high and low dose rates of 7.7 and 4.1 clones per 10^4 villi per gray, respectively. This dose sparing is attributable to repair of DNA damage at the lower dose rate.

Although mutation experiments can demonstrate DNA repair, very little is known about the spatial or temporal regulation of the different DNA repair pathways or how these change during differentiation.

3. SPATIAL ASPECTS OF CRYPT ORGANIZATION AND FUNCTION

All four intestinal cell types (columnar, Paneth, mucous and enteroendocrine) appear to have a common origin from a stem cell zone in the crypt base, which contains a population of undifferentiated cells. It is not known what proportion of these undifferentiated, crypt base columnar cells are stem cells. Only a small proportion of cell division occurs in the stem cell region. Most is located across the middle region (the proliferative zone) of the crypt as a consequence of a series of rapid amplifying transit divisions that originates with the daughters of stem cell division. A maturation zone near the top of the crypt contains no proliferative cells. Columnar, enteroendocrine and mucous cells reach the villus by progression through these zones as they migrate upwards with differentiated characteristics being gradually acquired as proliferative capacity is lost (Al-Dewachi *et al.* 1975; Bjerknes & Cheng 1981*a–e*). Thus, with the exception of Paneth cells, which are co-localized with the putative stem cell population, cell position in the crypt base defines the extent of progression along a differentiative/proliferative gradient.

Within this gradient cells respond differently to genotoxic insult. Apoptoses are induced by many genotoxic agents and these clearly tend to occur towards the crypt base either in the lower part of the proliferative zone or in the stem cell zone (Clarke *et al.* 1994; Merritt *et al.* 1994). Analysis of the distribution of radiation-induced apoptosis in p53-deficient and wild-type mice has demonstrated that the p53-dependent apoptoses after irradiation have a similar distribution and that this is correlated with a restricted lower crypt pattern of induction of p53. The determinants of survival over death in the lower crypt are not known, but are likely to include DNA repair processes. There are several different repair pathways including nucleotide and base excision repair (NER, BER) and mismatch repair (MMR); yet nothing is known about their relative contributions to repair in intestinal crypts or whether their activities are modulated along the differentiative gradient of the crypt.

The route of exposure of the intestine to environmental genotoxins may determine the frequency of induced mutations and this in turn may depend on the spatial pattern of induction of metabolizing enzymes. For example, benzo(a)pyrene (B(a)P), which is a potent small-intestinal mutagen, is three times more mutagenic to intestinal stem cells when delivered by the intraperitoneal (i.p.) as compared to the oral route. B(a)P requires metabolic activation to generate DNA-reactive species and the first step in this activation is primarily mediated by a member of the P450 family of enzymes, CYP1A1. This P450 enzyme is not normally expressed but is inducible in a wide range of tissues by several xenobiotics including B(a)P itself. After oral or i.p. administration, CYP1A1 is induced in intestinal villi or crypts, respectively. Thus, by using CYP1A1 induction as an indicator of exposure to B(a)P, it is clear that the crypt base population may be exposed to higher levels of B(a)P than cells at higher positions in the epithelium after i.p. treatment.

For these reasons the spatial pattern of DNA damage and repair in intestinal crypts may be important factors determining the risk of somatic mutation. Currently, there is no method of measuring the level of damage or rate of repair in different parts of intestinal crypts. We have attempted to develop such a method based on detection of DNA strand breaks.

4. STRAND BREAKS AND DNA REPAIR

During DNA repair by various pathways, including NER, BER and MMR, an important intermediate is a single DNA strand break. For NER this occurs during excision of a string of nucleotides containing a bulky adducting species. During MMR it occurs in the *de novo* (unmethylated) synthesized strand opposite the nearest methylated d(GATC) site (Modrich & Lahue 1996), whereas during BER it occurs subsequent to the action of DNA glycosylase (which generate apurinic/apyrimidinic sites) due to the action of an endonuclease.

Strand breaks arising during repair of the different pathways are short lived. To use them to measure DNA repair some method is needed to allow the cellular recognition and removal of damage but to block repair at the point of strand breakage. In this way, incomplete repair sites accumulate with time to the point that they are detectable. This is achievable for NER and BER using partly specific inhibitors. In NER, DNA polymerases α and δ are inhibited by aphidicolin (Wright *et al.* 1994), whereas in BER, DNA polymerase β is inhibited by incorporation of dideoxynucleotides (Singhal *et al.* 1995). (At present there is no specific inhibitor of MMR.) Actual or conditional (apurinic/apyrimidinic sites) strand breaks can also be caused directly by many agents, e.g. hydrogen peroxide.

Damage and repair can be discriminated by assaying strand breaks under appropriate conditions. Further, the

PHILOSOPHICAL TRANSACTIONS OF THE ROYAL SOCIETY B BIOLOGICAL SCIENCES

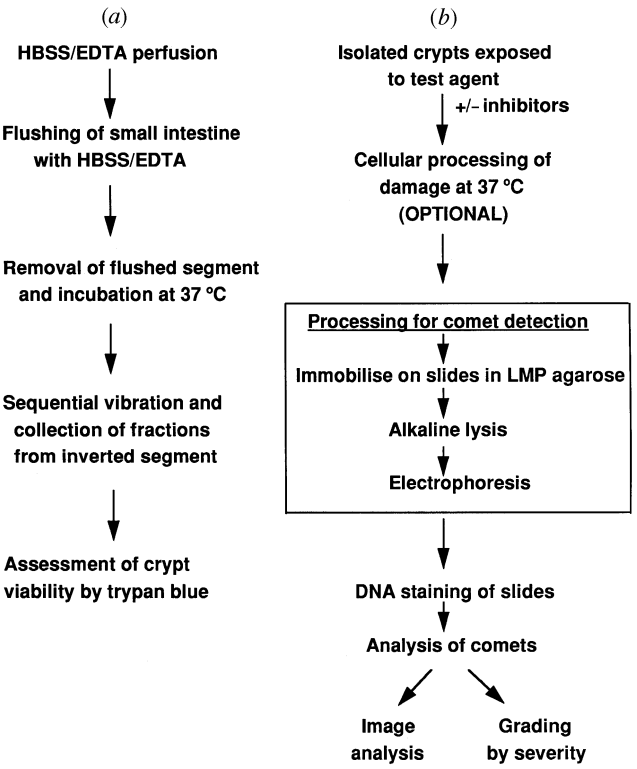

Figure 2. Flow chart showing the procedures for (*a*) crypt isolation, and (*b*) processing for the comet assay. HBSS/EDTA, Hepes balanced salt solution/ethylenediaminetetraacetic acid.

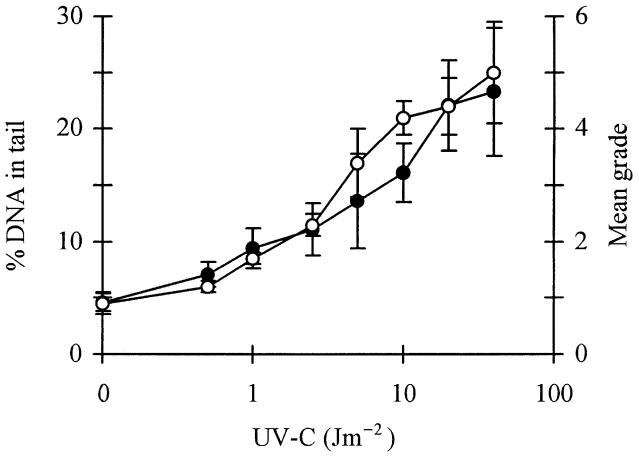

Figure 3. Dose responsiveness in the amount of DNA migrating from lysed crypts to form a comet tail after UV-C irradiation and incubation at 37 °C for 30 min in the presence of aphidicolin. Comets were measured by image analysis to give the percentage DNA in the tail (filled circles) or by visual grading (open circles).

contribution of a particular repair pathway can be defined by the choice of damaging agent and/or inhibitor used. For example, after UV irradiation of cells no direct strand breaks are induced and these accumulate only in the presence of aphidicolin during subsequent NER.

5. COMET ASSAY

An appropriate detection system must allow quantification of the response of different parts of intestinal crypts. A sensitive and quantitative method is the single-cell gel electrophoresis or 'comet' assay, which detects both single and double strand breaks. In the assay, strand breaks allow DNA to leave the comet head (the lysed nucleus) and migrate in an electrophoretic field to give rise to the comet tail. The value of the method is twofold. First, measurement of the relative amounts of DNA in the head versus the tail allows damage to be quantified (Olive *et al.* 1990*a*). Second, the damage is attributable to an individual cell. An important consequence of the latter is that subsets of cells differing in their responsiveness can be identified (Olive *et al.* 1990*b*).

The single-cell comet assay measures DNA strand breaks in individual cells that are either present as a dispersed population *in vivo* (e.g. haemopoietic cells, sperm) or obtained as such by enzymic digestion. In the assay, cells are exposed to a test agent and can either be allowed recovery times (during which they are incubated with DNA polymerase inhibitors to allow accumulation of strand breaks) or be processed for immediate detection of DNA strand breaks. Subsequently the cells are immobilized on a microscope slide in low melting point agarose, lysed under alkaline conditions and then electrophoresed and stained to visualize the DNA. Alkaline lysis permits unwinding of DNA and strand breaks allow DNA to leave the lysed nucleus (comet head) and migrate towards the anode (to form the comet tail).

Various methods can be employed to measure the relative amounts of DNA in the tail versus the head, which is directly related to the number of strand breaks (Gedik *et al.* 1992). Under the alkaline conditions of the assay, alkaline labile sites as well as frank strand breaks are detected.

6. CRYPT COMET ASSAY

The implications for modifying the single-cell assay for application to intestinal crypts is that intact crypts have to be isolated and processed for damage induction and repair with minimal levels of DNA damage in control crypts. After immobilization, alkaline lysis and electrophoresis, migrating DNA has to be measured and attributed if necessary to different regions of the crypt.

Intact murine crypts can be obtained by vascular perfusion with chelating agents and sequential vibration of intestinal segments (Bjerknes & Cheng 1981*f*; Brooks & Winton 1996) using the protocols indicated in figure 2.

The assay was first validated with UV-C irradiation, after which all strand breaks arise as a consequence of damage processing during repair. Crypts are incubated in aphidicolin to allow incomplete repair sites to accumulate. These initial studies demonstrated that isolated crypts could be maintained on ice for a period of several hours, and at 37 °C for up to one hour, before significant amounts of DNA migrated from control crypts on electrophoresis. Alkaline-lysed crypts and comets can be recognized under epifluorescence using 4′,6-diamidino-2-phenylindole (DAPI) to stain DNA. These have lost their cellular morphology but the crypt base and top can be identified. For each crypt the extent of comet formation can be measured either by detailed image analysis of a relatively few images or a grading system in which they

PHILOSOPHICAL TRANSACTIONS OF THE ROYAL SOCIETY B BIOLOGICAL SCIENCES

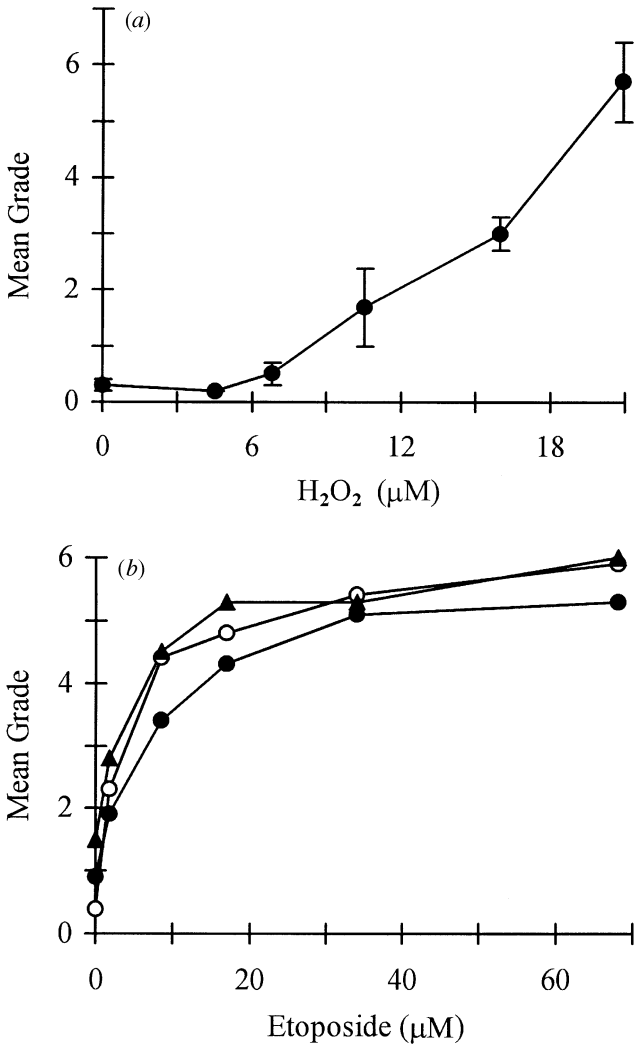

Figure 4. Dose responsiveness in the amount of DNA migrating from lysed crypts (by visual grading) to form a comet tail after treatment with (*a*) hydrogen peroxide (30 min, 4 °C), error bars show s.e.m.; and (*b*) etoposide for 5 min (filled circles), 15 min (open circles) and 30 min (filled triangles) at 37 °C.

are scored on a scale of 0–7. The advantage of the latter is that all crypts aligned perpendicular to the electophoretic field can be scored. Using either method, dose responsiveness can be demonstrated in the amount of DNA migrating from UV-C-irradiated crypts incubated with aphidicolin for 30 min (figure 3).

To allow analysis of zones of the crypt, approximating stem, proliferative and maturation zone, some account had to be taken of differences in point of fracture of crypts during isolation, which would tend to remove an unknown amount of the maturation zone. To achieve this we measured the length taken to comprise the stem cell zone (cell positions 1–4 from the crypt base), the proliferative zone (positions 5–17) and maturation zone (positions 18–top) in sections stained with haemotoxylin and eosin. These micrometer lengths were translated into pixel values for 20 clearly intact isolated crypts (after alkaline lysis and DAPI staining) using image analysis software. These values were taken as absolute pixel values in subsequent analyses to determine the stem and proliferative zones, with the maturation zone being taken as the length remaining at the crypt top.

7. DAMAGE KINETICS

Appropriate damage kinetics after treatment with different agents is necessary to validate the assay. For example, two test agents, hydrogen peroxide and etoposide, cause crypt comet formation in a dose-responsive manner as indicated by increasing amounts of DNA migrating from the crypt (figure 4*a*,*b*). Hydrogen peroxide induces frank strand breaks and alkaline labile sites via a direct interaction between free radicals and DNA. Hydrogen peroxide is damaging at 4 °C and there is a direct relationship between the concentration of hydrogen peroxide and the amount of damage (figure 4*a*). Etoposide acts by binding topoisomerase II at the site of topoisomerase II-induced strand breaks and preventing release and religation of DNA. Consequently, the effect of etoposide is saturable with time, as strand breaks occur in the presence of the drug only until all topoisomerase II molecules are arrested at the site of breaks (figure 4*b*). This occurs more quickly at higher rather than lower drug doses.

8. COMET ASSAY AND ROUTES OF INTESTINAL MUTAGENESIS

The human diet contains many potentially carcinogenic substances including heterocyclic amines such as 2-amino-1-methyl-6-phenylimidazo[4,5-*b*]pyridine (PhIP) and polycyclic aromatic hydrocarbons such as B(a)P. These require metabolic activation to generate reactive species in order to damage DNA. Both chemicals are potent small-intestinal mutagens as indicated by the *Dlb*-1 assay (Brooks *et al.* 1994; D. J. Winton and R. A. Brooks, unpublished data). One question that arises is whether mutation arises via the local generation of damaging metabolites by the crypt epithelium (and stem cell population) themselves or whether it occurs by their delivery from distant sites?

PhIP requires an initial activation step by CYP1A2, a member of the cytochrome P450 family, to generate N-OHPhIP, which is a weak direct-acting genotoxin. However, the ultimate electrophilic species probably results from esterification of N-OHPhIP by either sulphation or acetylation. The small-intestinal epithelium contains significant amounts of acetyltransferase and sulphotransferase enzymes (Timbrell 1992), although the spatial distribution of these have not been described. We have previously argued that stem cell mutation by PhIP arises by delivery of reactive metabolites (notably N-OHPhIP) from the liver via the circulation. This is partly based on the cellular distribution of CYP1A2 in the mouse. It is constitutively expressed in the liver where it is inducible by β-naphthoflavone and 3-methylcholanthrene (but not PhIP itself) but is absent from the intestinal crypt epithelium. (Some CYP1A2 is found on a few sporadically distributed cells on the villus epithelium of the proximal small intestine.)

A prediction arising from this interpretation is that a product of liver metabolism is able to induce DNA damage in intestinal crypts, which is testable using the crypt comet assay. In preliminary experiments, we have been able to demonstrate that the assay can detect damage induced by N-OHPhIP in a dose-responsive manner (figure 5*a*). In a second experiment, we incubated

PHILOSOPHICAL TRANSACTIONS OF THE ROYAL SOCIETY B BIOLOGICAL SCIENCES

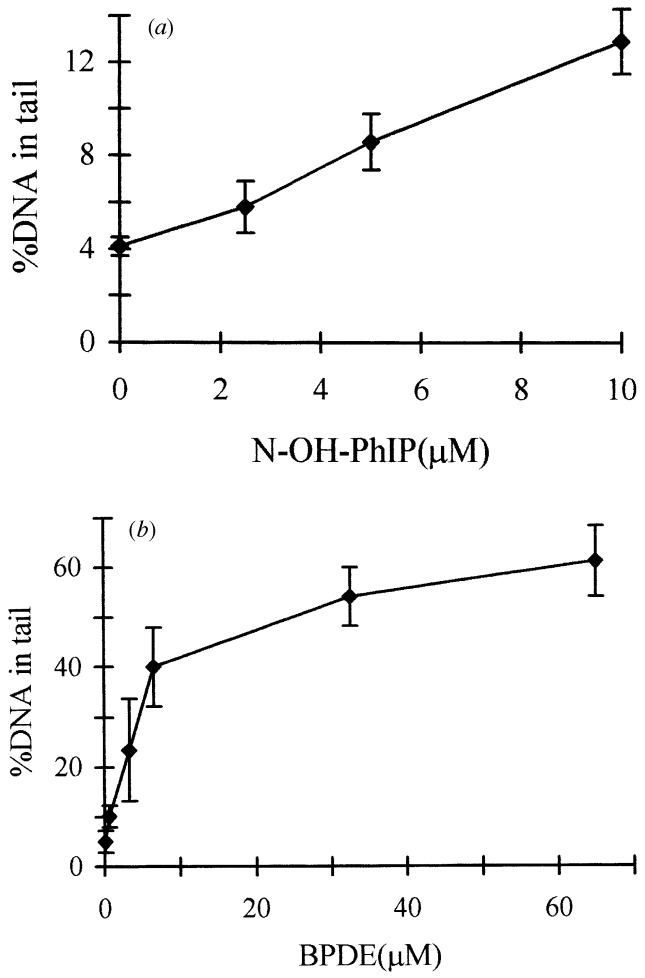

Figure 5. Dose responsiveness in the amount of DNA migrating from lysed crypts (by image analysis) to form a comet tail after treatment with (*a*) N-OHPhIP (30 min at 37 °C), and (*b*) B(a)P 7,8 diol 9,10 epoxide (*anti*) BPDE (30 min at 37 °C). The plateau observed with BPDE is probably due to a maximal effect in the assay due to the bulk of DNA leaving the crypt on electrophoresis. Error bars show s.e.m.

Table 1. *Comet formation from PhIP-treated crypts*

treatment[a]	total crypts analysed	% DNA in comet tail[b]	s.d.
control[c]	20	4.5	0.9
microsomes[d]	20	4.5	1.2
PhIP[e]	20	6.3	1.0
PhIP+microsomes	20	11.5	3.6

[a] Aphidicolin (30 μM) was included in all treatment groups.
[b] Mean of four experiments.
[c] Solvent (DMSO) only.
[d] Isolated from livers of mice pre-induced with 3-methyl cholanthrene (80 mg kg^{-1}).
[e] Concentration, 450 μM.

crypts with PhIP and aphidicolin only or together with liver microsomes isolated from mice induced for CYP1A2 by 3-methylcholanthrene. PhIP in the presence of microsomes showed a two- to threefold increase in comet formation compared with control groups (table 1). These experiments demonstrate that the crypt comet assay can provide a functional test to detect the product of CYP1A2 metabolism (i.e. N-OHPhIP). This may be by direct interaction or following esterification by acetyltransferases or sulphotransferases present in the crypt epithelium. Further, reactive species can be generated from PhIP entirely *in vitro* by providing appropriate liver metabolism (and presumably CYP1A2) in the form of a liver microsome fraction. These results are in accord with a mechanism of stem cell mutation by PhIP after delivery of reactive metabolites from the liver.

Table 2. *Effect of β-naphthoflavone induction of CYP1A1 on formation of B(a)P-induced comets*

(Mice were i.p. injected with either 80 mg kg^{-1} β-naphthoflavone or corn oil, 48 h and 6 h before isolation of crypts.)

	dose[a] (μM)	total crypts analysed	% DNA in comet tail[b]
control[c]	0	10	4.4
	12.5	10	5.9
	25	10	7.7
	50	10	7.6
	100	10	8.4
β-NF[d]	0	20	4.1
	12.5	15	5.6
	25	15	6.9
	50	15	8.1
	100	25	8.6

[a] Dose of B(a)P; 30 μM aphidicolin was incubated in all groups.
[b] Mean of two and three experiments for control and β-naphthoflavone-induced groups, respectively.
[c] Received DMSO solvent only.
[d] β-naphthoflavone.

The first step in the activation of B(a)P is commonly thought to be mediated by CYP1A1. This enzyme is not normally expressed but is inducible in responsive mouse strains via the *Ah* locus by several xenobiotics including B(a)P itself. After i.p. administration it is induced in the crypt epithelium. However, in a comparison of B(a)P-induced *Dlb-1* mutation frequencies in *Ah*^{b} responsive mice with *Ah*^{d} non-responsive mice (inducible or non-inducible for CYP1A1 respectively) we were able to show that around 45% of the mutagenic responsiveness observed in responders could be induced in non-responders (and therefore in the absence of CYP1A1) at the same treatment dose of B(a)P. This indicates that some proportion of the mutations in responder mice may be attributable to a route of activation that is independent of CYP1A1. The activation of B(a)P involves two epoxidation steps. The first, in which CYP1A1 is most strongly implicated, generates a 7,8 epoxide that, after hydrolysis, forms a 7,8 diol 9,10 epoxide. To investigate the involvement of crypt epithelial CYP1A1 we first confirmed that the diolepoxide (BPDE) is capable of inducing damage in the crypt assay (figure 5*b*). In fact, BPDE caused extensive damage when incubated directly with crypts, confirming that this product of CYP1A1 metabolism is detectable in the assay. Subsequently, we have incubated B(a)P (and aphidicolin) with crypts isolated from uninduced mice or mice treated with i.p. injections of β-naphthoflavone to induce crypt expression of CYP1A1. This experiment demonstrated a small dose-dependent increase in comet

PHILOSOPHICAL TRANSACTIONS OF THE ROYAL SOCIETY B BIOLOGICAL SCIENCES

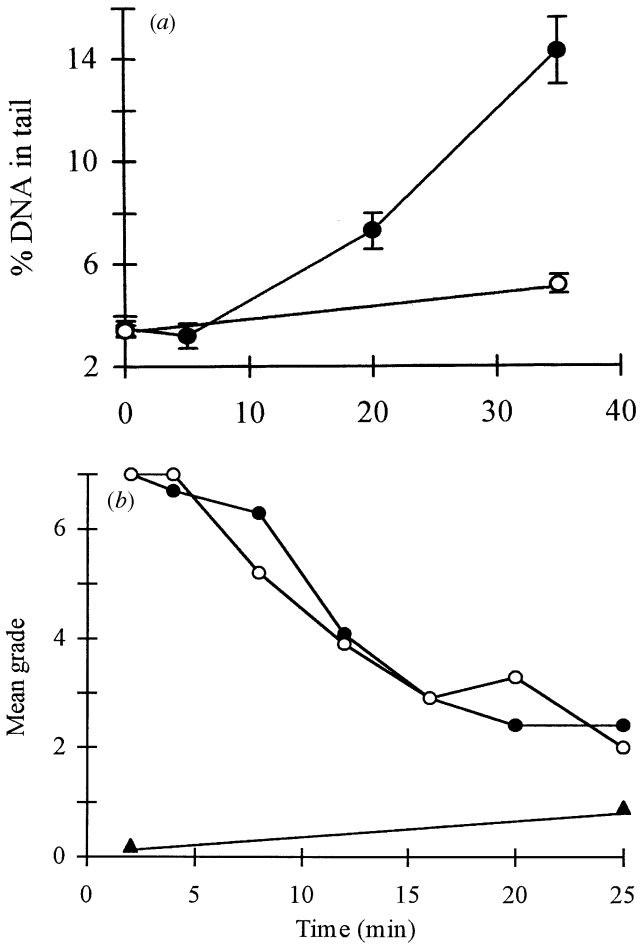

Figure 6. Demonstration of repair competence of isolated crypts after damage: (*a*) UV-C irradiation (10 J m^{-2} incubated at 37 °C with 30 μM aphidicolin), quantification by image analysis, error bars show s.e.m.; (*b*) gamma irradiation (15 Gy, 37 °C), quantification by visual grading. Two individual experiments are shown: (*a*) incomplete repair sites accumulate after UV-C irradiation in the presence of aphidicolin; (*b*) after gamma irradiation, frank or conditional strand breaks are rapidly repaired causing decreased amounts of DNA to migrate.

formation in both cases but with no difference between the two groups (table 2). Taken together with the mutation data this may indicate that CYP1A1 induced in the crypt base does not contribute to the generation of reactive electrophiles from B(a)P. Instead there may be a CYP1A1-independent route for activation of B(a)P in the crypt epithelium.

9. REPAIR USING THE COMET ASSAY

The repair competence of isolated crypts is demonstrable by two different categories of experiment, i.e. by the induction of strand breaks subsequent to damage or their resolution. After UV-C and gamma irradiation an equal distribution of DNA damage along the crypt can be assumed. However, with UV-C irradiation, as described previously, strand breaks occur with time in the presence of aphidicolin (figure 6*a*). In mouse cells repair of UV damage can take up to 24 h. Thus the experiments described here show only the initial NER activity, with the residual damage being unresolved over the time of

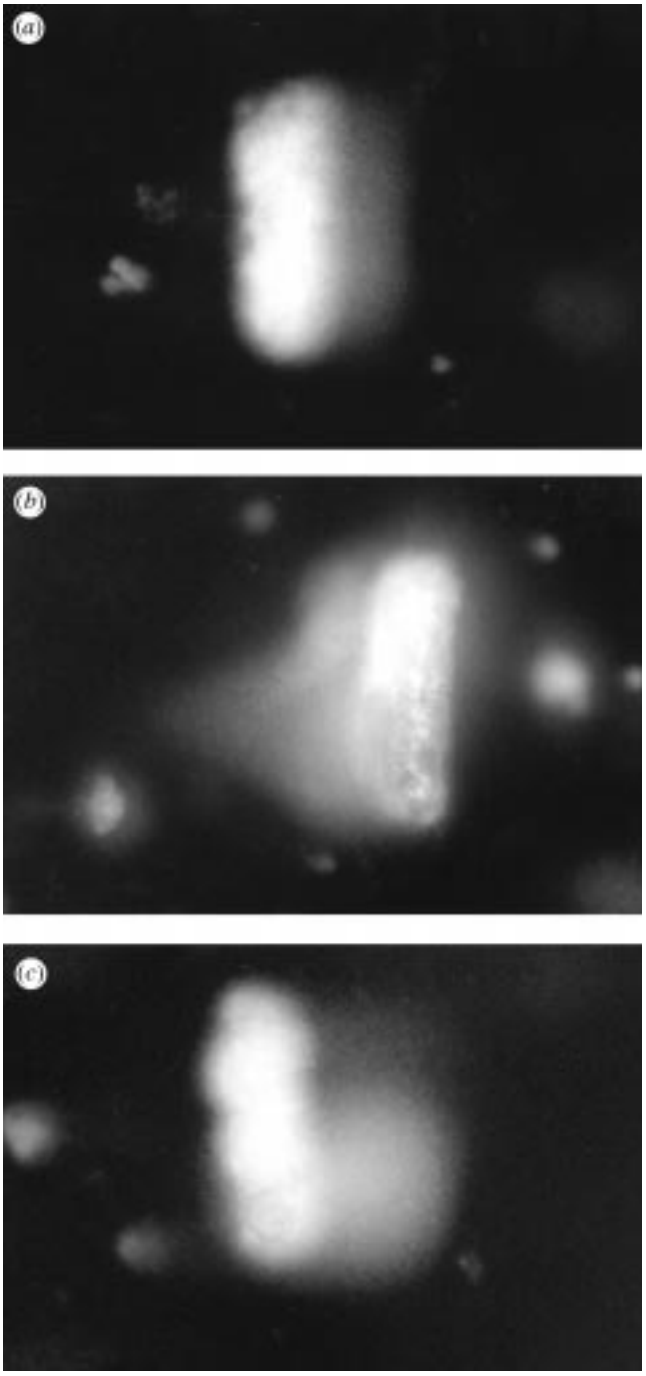

Figure 7. Crypt comets induced by different genotoxic agents: (*a*) UV-C (20 J m^{-2}); (*b*) etoposide (68 μM); (*c*) hydrogen peroxide (6.8 μM).

the experiment. No increase in comet formation over control was observed in UV-irradiated crypts not subsequently incubated with aphidicolin. In contrast, after gamma irradiation all damage is visualized in the earliest time point and subsequent repair is identified by the decrease in the proportion of DNA migrating with time (figure 6*b*). Unlike UV-C, repair of damage after gamma irradiation is allowed to go to completion by removal of damaged bases, incorporation of nucleotides and ligation.

10. SPATIAL ASPECTS OF CRYPT RESPONSIVENESS

After UV-C irradiation and incubation with aphidicolin, all regions of the crypt contribute equally to form

PHILOSOPHICAL TRANSACTIONS OF THE ROYAL SOCIETY B BIOLOGICAL SCIENCES

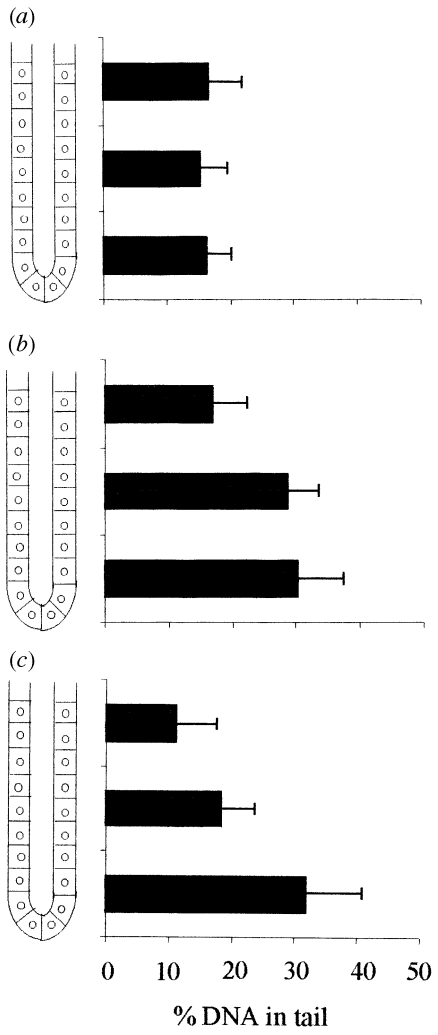

Figure 8. Schematic representation of the percentage DNA in the comet tail arising from the base, middle and top of crypts for (*a*) UV-C, (*b*) etoposide, and (*c*) hydrogen peroxide (6.8 μM). (*b*, *c*) Mean±s.e.m. of 11 images, (*a*) mean±s.e.m. of seven images.

the comet tail (figures 7 and 8). In the single-cell assay, accumulation of strand breaks in the absence of aphidicolin is only observed in cells with low nucleotide pool (Green *et al.* 1992). Consequently, with the caveat regarding the proportion of UV-C damage repaired, cells at all positions in the crypt appear to contain sufficient nucleotide pools for DNA repair synthesis over the time of the experiment. Similarly, after gamma irradiation all positions in the crypt appear equally repair competent.

Lower doses of hydrogen peroxide (below 6.8 μM) induced comet formation preferentially from the lower crypt (figures 7 and 8). At high concentrations all regions of the crypt appeared to respond equally. This enhanced responsiveness of the lower crypt may indicate a greater bioavailibility of transition metal ions in this region, which promotes radical production from hydrogen peroxide. Alternatively there may be greater antioxidant protection in the upper crypt, which is only overcome at higher concentrations. This obviously requires further study, particularly to determine which cell population in the crypt base (Paneth cells or crypt base columnar cells) are responsible for the effect.

All doses of etoposide produced a positional effect in crypt comets (figures 7 and 8). An apparent double comet tail was induced, one running parallel to the edge of the crypt and another tapered tail extending from the lower half of the crypt. The location of the apex of the latter was estimated (with respect to cell position from the crypt base) as extending from cell position 9, which falls well within the proliferative compartment. This suggests that there is a gradual change by cell position in the amount of active topoisomerase II. Intriguingly, however, this does not explain the tapered nature of the comet tail, which would seem to require a qualitative difference in the pattern of strand breakage.

11. SUMMARY

The crypt comet assay has the ability to distinguish spatial patterns of DNA damage and therefore to detect differences in the clearance of damage by DNA repair in different regions of the crypt.

The assay is still in an early stage of its development and two challenges for the future will be: (i) to prolong the useful *in vitro* life of intestinal crypts; and (ii) to move from observation of phenomena to an understanding of the mechanistic basis for the spatial differences being observed.

The first of these may require relatively simple procedural modifications (e.g. inclusion of protein or serum in all solutions). However, if the *in vitro* life is not extendable, the assay will still be useful. For example, if complete repair of UV-C damage cannot be followed *in vitro* should be possible to follow repair induced *in vivo* (e.g. by B(a)P) and monitor NER by taking a series of sampling windows by isolating crypts from a cohort of treated animals with time.

The second goal of understanding the mechanistic basis for spatial differences may, at least in part, be achieved by development of the assay itself. In the single-cell assay, comet tail formation from proliferative and non-proliferative cells can be distinguished by visualizing comets from cells that have incorporated BrDU using a FITC-conjugated antibody. In preliminary experiments we have identified individual FITC-labelled cells contributing to UV-C-induced crypt comets after i.p. injection of BrDU shortly before crypt isolation. Application of this methodology should allow the cells contributing to the lower crypt damage, observed at lower concentrations of hydrogen peroxide, to be identified. (Paneth cells will remain unlabelled in 'flash labelling' studies, while a proportion of the crypt base columnar cells will incorporate BrDU).

The assay may also have an important role in determining if carcinogens that are intestinal mutagens achieve their mutagenic effect by a direct localized interaction with the crypt epithelium. Generation of strand breaks on incubation of test compounds with crypts would be a strong indicator of metabolism within crypt cells. A problem here may be false negatives due to the complexity of activation pathways. The crypt epithelium may only be capable of a limited repertoire of metabolizing steps such that they can generate only the initial or final step in the generation of electrophilic reactive species.

PHILOSOPHICAL TRANSACTIONS OF THE ROYAL SOCIETY B BIOLOGICAL SCIENCES

In other respects the crypt assay can develop in directions indicated by the single-cell assay. These include discrimination of double strand breaks by performing the assay under neutral conditions, and recognition of repair by specific DNA lesions using purified DNA repair enzymes to induce enzymic cleavage in permeabilized cells.

The spatial and temporal regulation of DNA repair processes in complex tissues is much ignored and the intestine provides a good model. The extended resources and reagents that exist in the field of DNA repair and the quantification of the spatial pattern of strand breaks in the crypt comet assay provides a powerful method to explore determinants of damage and modulation of repair processes accompanying differentiation in the intestinal crypt.

D.J.W. is supported by a programme grant from the Cancer Research Campaign (CRC).

REFERENCES

Al-Dewachi, H. S., Wright, N. A., Appleton, D. R. & Watson, A. J. 1975 Cell population kinetics in the mouse jejunal crypt. *Virchows Arch. Cell Path.* **18**, 225–242.

Bjerknes, M. & Cheng, H. 1981*a* The stem cell zone of the mouse small intestinal epithelium. I. Evidence from Paneth cells in the adult mouse. *Am. J. Anat.* **160**, 51–64.

Bjerknes, M. & Cheng, H. 1981*b* The stem cell zone of the small intestinal epithelium. II. Evidence from Paneth cells in the new-born mouse. *Am. J. Anat.* **160**, 65–76.

Bjerknes, M. & Cheng, H. 1981*c* The stem cell zone of the small intestinal epithelium. III. Evidence from columnar, enteroendocrine, and mucous cells in the adult mouse. *Am. J. Anat.* **160**, 76–92.

Bjerknes, M. & Cheng, H. 1981*d* The stem cell zone of the small intestinal epithelium. IV. Effects of resecting 30% of the small intestine. *Am. J. Anat.* **160**, 93–104.

Bjerknes, M. & Cheng, H. 1981*e* The stem cell zone of the small intestinal epithelium. V. Evidence for controls over orientation of boundaries between the stem cell zone, proliferative zone and maturation zone. *Am. J. Anat.* **160**, 105–112.

Bjerknes, M. & Cheng, H. 1981*f* Methods for the isolation of intact epithelium from the mouse intestine. *Anat. Rec.* **199**, 565–574.

Brooks, R. A. & Winton, D. J. 1996 Determination of spatial patterns of DNA damage and repair in intestinal crypts by multi-cell gel electrophoresis. *J. Cell. Sci.* **109**, 2061–2068.

Brooks, R. A., Gooderham, N. J., Zhao, K., Edwards, R. J., Howard, L. A., Boobis, A. R. & Winton, D. J. 1994 2-amino-1-methyl-6-phenylimidazo [4,5-*b*]pyridine is a potent mutagen in the mouse small intestine. *Cancer Res.* **54**, 1665–1671.

Clarke, A. R., Gledhill, S., Hooper, M. L., Bird, C. C. & Wyllie, A. H. 1994 p53 dependence of early apoptic and proliferative responses within the mouse intestinal epithelium following γ-irradiation. *Oncogene* **9**, 1767–1773.

Fu, K. K., Phillips, T. L., Kare, L. J. & Smith, V. 1975 Tumour and normal tissue response to irradiation *in vivo*: variation with decreasing dose rates. *Radiat. Res.* **114**, 709–716.

Gedik, L. M., Ewen, S. W. B. & Collins, A. R. 1992 Single-cell gel electrophoresis applied to the analysis of UV-C damage and its repair in human cells. *Int. J. Radiat. Biol.* **62**, 313–320.

Green, M. H. L., Lowe, J. E., Harcourt, S. A., Akinluyi, P., Rowe, T., Cole, J., Anstey, A. V. & Arlett, C. F. 1992 UV-C sensitivity of unstimulated and stimulated human lymphocytes from normal and xeroderma pigmentosum donors in the comet assay: a potential diagnostic technique. *Mutat. Res.* **273,** 137–144.

Harvey, M., McArthur, M. J., Montgomery, C. A., Butel, J. S., Bradley, A. & Donehower, L. A. 1993 Spontaneous and carcinogen-induced tumorigenesis in p53-deficient mice. *Nat. Genet.* **5**, 225–229.

Harvey, M., Vogel, H., Lee, E. Y., Bradley, A. & Donehower, L. 1995 Mice deficient in both p53 and Rb develop tumors primarily of endocrine origin. *Cancer Res.* **55**, 1146–1151.

Hu, N., Gutsmann, A., Herbert, D. C., Bradley, A., Lee, W. H. & Lee, E. Y. 1994 Heterozygous Rb-1 delta 20/+ mice are predisposed to tumors of the pituitary gland with nearly complete penetrance. *Oncogene* **9**, 1021–1027.

Huczkowski, J. & Trott, K. R. 1984 Dose fractionation effects in low dose rate irradiation of jejunal crypt stem cells. *Int. J. Radiat. Biol.* **46**, 293–298.

Ito, N., Hasegawa, R., Sano, M., Tamano, S., Esumi, H., Takayama, S. & Sugimura, T. 1991 A new colon and mammary carcinogen in cooked food, 2 amino-1-methyl-6-phenylimidazo[4,5-b]pyridine (PhIP). *Carcinogenesis* **12**, 1503–1506.

Jacks, T., Remington, L., Williams, B. O., Schmitt, E. M., Halachmi, S., Bronson, R. T. & Weinberg, R. A. 1994 Tumor spectrum analysis in p53-mutant mice. *Curr. Biol.* **4**, 1–7.

Merritt, A. J., Potten, C. S., Kemp, C. J., Hickman, J. A., Balmain, A., Lane, D. P. & Hall, P. A. 1994 The role of *p53* in spontaneous and radiation-induced apoptosis in the gastrointestinal tract of normal and *p53*-deficient mice. *Cancer Res.* **54**, 614–617.

Modrich, P. & Lahue, R. 1996 Mismatch repair in replication fidelity, genetic recombination and cancer biology. *A. Rev. Biochem.* **65**, 101–133.

Olive, P. L., Banath, J. P. & Durand, R. E. 1990*a* Heterogeneity in radiation-induced DNA damage and repair in tumor and normal cells measured using the 'comet' assay. *Radiat. Res.* **122**, 86–94.

Olive, P. L., Banath, J. P. & Durand, R. E. 1990*b* Detection of etoposide resistance by measuring DNA damage in individual chinese hamster cells. *J. Natn. Cancer Inst.* **82**, 779–783.

Potten, C. S., Schofield, R. & Lajtha, L. G. 1979 A comparison of cell replacement in bone marrow, testis and three regions of surface epithelium. *Biochim. Biophys. Acta* **560**, 281–289.

Purdie, C. A. (and 10 others) 1994 Tumour incidence, spectrum and ploidy in mice with a large deletion in the p53 gene. *Oncogene* **9**, 603–609.

Singhal, R. K., Prasad, R. & Wilson, S. H. 1995 DNA polymerase β conducts the gap-filling step in uracil-initiated base excision repair in a bovine testis nuclear abstract. *J. Biol. Chem.* **270**, 949–957.

Timbrell, J. A. 1992 *Principles of biochemical toxicology*, 2nd edn, chap. 4, pp. 73–124. London and Washington: Taylor & Francis.

Winton, D. J., Peacock, J. H. & Ponder, B. A. J. 1989 Effect of gamma radiation at high- and low-dose rate on a novel *in vivo* mutation assay in mouse intestine. *Mutagenesis* **4**, 404–406.

Wright, G. E., Hubscher, U., Khan, N. N., Focher, F. & Verri, A. 1994 Inhibitor analysis of calf thymus DNA polymerases α, δ and ε. *FEBS Lett.* **341**, 128–130.